D.-J. Luo^{1,2}, H.-J. Shao², F.-J. Wei², K.-Z. Zhang², Z.-Y. Cui², J. Yu², S.-H. Qin²*

Morphology and Isothermal Crystallization Kinetics of Polypropylene/ Poly(ethylene-co-vinyl alcohol) Blends

Polypropylene (PP)/poly(ethylene-co-vinyl alcohol) (EVOH) blends were prepared by melt blending using PP-g-MAH as a compatabilizer. The microstructure and rheological behavior of PP/EVOH blends were studied. The results showed the that EVOH particles were uniformly dispersed in the PP matrix and inhibited the mobility of PP chains. The isothermal crystallization kinetics and morphology development of PP/EVOH blends were compared with that of pure PP. It was found that the EVOH essentially acted as an effective nucleating agent for PP, which could significantly increase the nucleation rate because the EVOH molecules in PP/EVOH blends aggregated together to form interface. Therefore, the introduction of EVOH increased the overall rate of isothermal crystallization compared with pure PP, although the PP molecular chains would be hindered seriously if excessive amounts of EVOH were added. X-ray diffraction showed that pure PP and PP/ EVOH blends exhibited an identical crystal structure, and the crystallinity of the PP phase in the blends was not significantly different from that of pure PP.

1 Introduction

Semi-crystalline polypropylene (PP) is one of suitable materials for hollow fiber membranes due to its outstanding advantages, e.g. low cost, easy processing, good mechanical properties, chemical stability, and non-toxicity (Saffar et al., 2014). PP hollow fiber membranes are important in membrane separation technology and widely used in many fields, e.g., pretreatment of seawater, waste-water treatment, gas separation, petroleum chemical industry and biomedical applications (Saffar et al., 2014; Baker, 2004). Though PP hollow fiber membranes prepared by melt spinning and cold-stretching (MSCS) have high strength, we found that a lot of hole-channels of the membrane clog. The closure phenomenon reduces the water flux of the membrane. We design a membrane with a lot of three-di-

E-mail: caiyuanzhangting@126.com

mensional circular structures in the interior of the membrane wall which was fabricated through blending PP with poly(ethylene-co-vinyl alcohol) (EVOH) and fiber spinning followed by stretching. The three-dimensional circle structure with the function of traffic circle is designed according to the principle of two phase separation (Li et al., 2011; Mei et al., 2002). This structure will effectively solve the closure phenomenon of hole-channels in theory.

However, the crystalline structure of the precursor hollow fibers is the key factor in the first step of the preparation of hollow fiber membrane by MSCS. It has been reported that the addition of heterogeneous materials (impurities, nucleating agent, or others) would change the crystallization mechanism of PP (Naffakh et al., 2008; Fan et al., 2015; Gupta et al., 2013; Zhang et al., 2014; Zhou et al., 2010). Therefore, it is important to find out how EVOH will affect the crystallization behavior of PP with maleic anhydride-grafted polypropylene (PP-g-MAH) as compatibilizer. Moreover, the practical preparation process of PP/EVOH hollow fiber membranes involves crystallization conditions that are analogous to isothermal crystallization. Thus, understanding the crystallization kinetics of PP/EVOH blends under isothermal conditions is very crucial from a scientific perspective. In this study, the effects of EVOH on the morphology and crystallization kinetics of PP/EVOH blends will also be investigated. The results of this investigation will be used to develop a membrane processing model for a larger study of the development of hollow fiber membranes prepared by MSCS with three-dimensional circlular structure.

2 Experimental

2.1 Materials

Homopolymer PP T30S with a melt index of 2.5 to 3.5 g/ $10 \, \text{min}$ is supplied by Dushanzi petrochemical company (Xinjiang, China). The melting point, T_m , of the resins obtained by differential scanning calorimetry is $166\,^{\circ}\text{C}$. EVOH (L171B) with a melt index of 4 g/10 min is obtained from Kuraray (Japan). The content of vinyl is 27 mol%. As compatibilizer, PP-g-MAH (CA100) with a grafting degree of 1 %, was purchased from Arkema, Paris, France.

¹Department of Polymer Material and Engineering, College of Materials and Metallurgy, Guizhou University, Guiyang, PRC ²National Engineering Research Center for Compounding and Modification of Polymeric Materials, Guiyang, PRC

^{*} Mail address: Shuhao Qin, National Engineering Research Center for Compounding and Modification of Polymeric Materials, Guiyang 550014, PRC

2.2 Sample Preparation

Firstly, all the raw materials were adequately dried in a vacuum oven at $80\,^{\circ}\text{C}$ for 24 h and mixed according to the compositions presented in Table 1. Then the blends were extruded on a SHJ-50 twin-screw extruder, Nanjing Jieya Extrusion Equipment Co., Ltd., Nanjing, PRC, (L/D = 48, D = 42 mm) at 215 $^{\circ}\text{C}$ with the screw rotational speed of 160 r/min. Finally, all pellet samples from the extruder were dried for 12 h at $80\,^{\circ}\text{C}$.

2.3 Characterization

2.3.1 Field Emission Scanning Electron Microscope

Quanta FEG250 (FESEM) of FEI, Oregon, USA, was employed to observe the surfaces of pure PP and PP/EVOH blends. All samples were quenched in liquid nitrogen.

2.3.2 Rotational Rheometer

Dynamic rheological measurements were performed on a rotational rheometer (ARES-G2, TA Instruments, New Castle, USA). The type of rheometer plates used was parallel-plates and with a diameter of 25 mm. The dynamic viscoelastic properties were determined with temperature ranging from 220 to $130\,^{\circ}\text{C}$. The cooling rate was $5\,^{\circ}\text{C/min}$, and the strain value was $5\,\%$.

2.3.3 Differential Scanning Calorimetry

A differential scanning calorimeter (DSC), model A-Q10 from TA Instruments, was used to study the crystallization behavior of blends under a nitrogen atmosphere. For non-isothermal tests, samples of about 5 to 8 mg were used. The thermal history of the samples was eliminated by heating the samples at 220 °C for a period of 5 min. Non-isothermal crystallization was measured at a cooling rate of 10 °C/min. The crystallization curve was recorded. For isothermal tests, samples of about 5 to 8 mg were used. The isothermal crystallization was measured at various isothermal crystallization temperatures (T_C).

Sample	PP %	PP-g-MAH %	EVOH %
Pure PP	100	0	0
PP-g-MAH	0	100	0
EVOH	0	0	100
PP/EVOH10	90	0	10
EVOH-0	100	5	0
EVOH-5	95	5	5
EVOH-10	90	5	10
EVOH-15	85	5	15

Table 1. Compositions of the PP/EVOH blends

The samples were rapidly cooled to T_C and held at T_C for a period of time until complete crystallization. Subsequently, samples were cooled to $40\,^{\circ}C$ and held at $40\,^{\circ}C$ for 5 min. Finally, the samples were heated to $220\,^{\circ}C$ at $10\,^{\circ}C/min$ rate again. The crystallization curves and the second melting curves were recorded.

2.3.4 Polarized Light Microscopy(PLM)

Morphological observations of various samples were performed using a polarized light microscope (model XP-P, Sunny Optical Technology Co., Ltd., Ningbo, PRC). The extruded granules of about 3 mg were melted at 250 °C on the hot stage, and squeezed to obtain thin films. Then, the films were heated to 250 °C and held for 5 min. Finally, the films were cooled to 155 °C and held at 155 °C for a period of time until complete crystallization. Subsequently morphological photographs of crystallization were recorded with the aid of a digital camera.

2.3.5 X-Ray Diffraction

The X-ray diffraction (XRD) analysis was performed using a D/Max-RA X-ray diffractometer (Bruker Daltonics Inc., Massachusetts, USA) at room temperature. The copper- K_{α} radiation source was operated at 35 kV and 25 mA, and the patterns were recorded by monitoring the diffractions from 2° to 45° at the scanning speed of 3° min⁻¹.

3 Results and Discussion

3.1 Microstructural and Viscoelastic Properties of PP/EVOH Blends

Figure 1 presents the FE-SEM images of the cross-section of pure PP and PP/EVOH blends. The sea-island structure is not observed in the pure PP and EVOH-0. However, it is clearly observed in EVOH-5, EVOH-10 and EVOH-15, and the number of sea-island increases with the increase of the amount of EVOH. The separated two-phase interface is not observed, indicating that the compatibility of the PP and EVOH is improved. Moreover, the EVOH particles exhibit an average particle size of 0.5 to 2.0 μm and uniformly disperse in the PP matrix.

The complex viscosity of the pure PP and PP/EVOH blends at different temperatures are shown in Fig. 2. The complex viscosity of all samples increases with the decrease of temperature. The complex viscosity of EVOH-5 and EVOH-10 are higher than that of pure PP between 170 and 200 °C. The complex viscosity of EVOH-15 is higher than that of pure PP below 200 °C. The complex viscosity of EVOH-5, EVOH-10 and EVOH-15 are proportional to the amount of EVOH added. The results show that the added EVOH inhibits the molecular mobility of PP, and the more EVOH is added, the more inhibition there is.

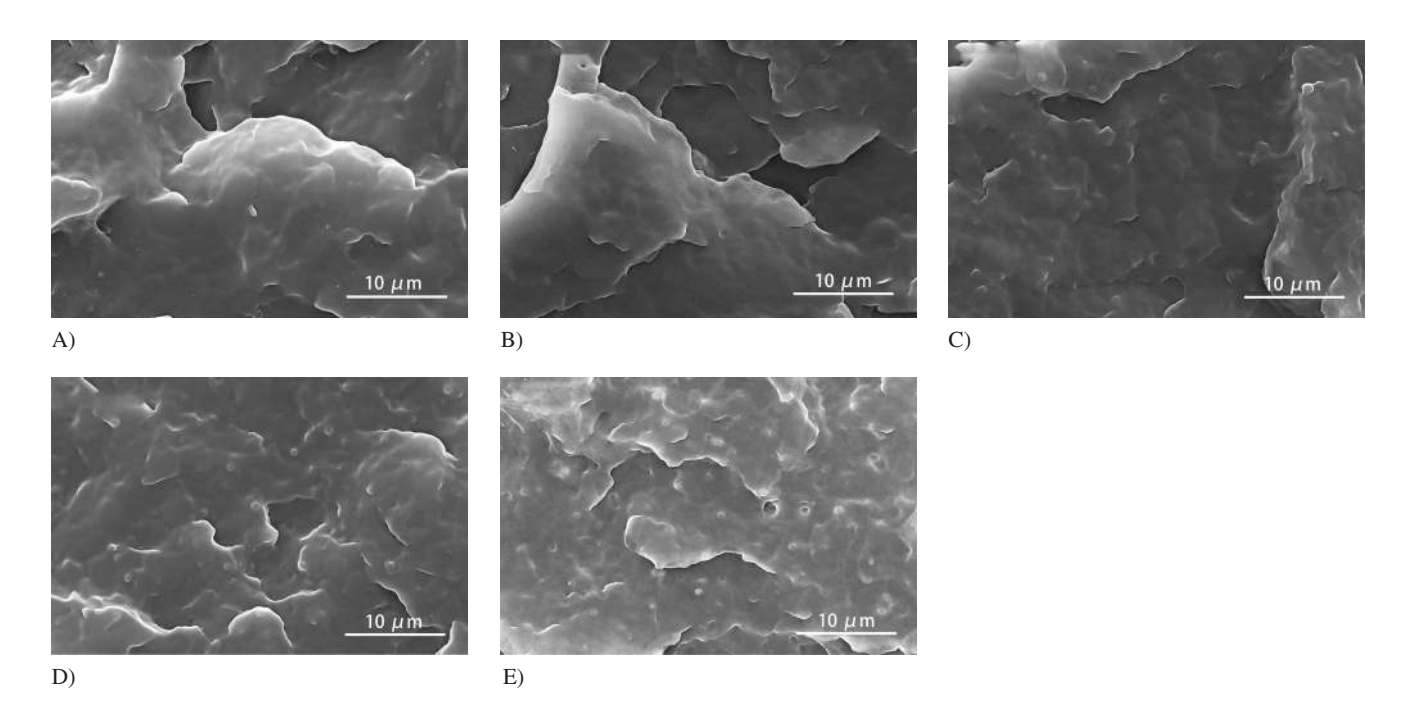


Fig. 1. FE-SEM images of the cross-section of pure PP and PP/EVOH blends, A) pure PP, B) EVOH-0, C) EVOH-5, D) EVOH-1, E) EVOH-15

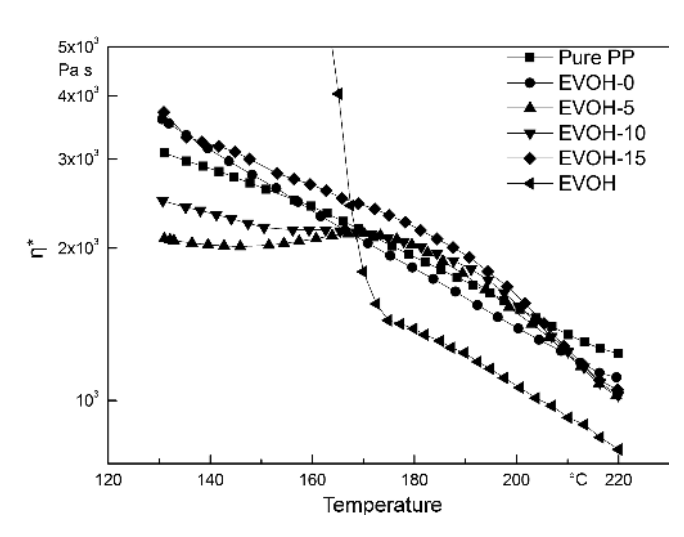


Fig. 2. Complex viscosity of pure PP and EVOH and PP/EVOH blends at different temperatures

3.2 Non-Isothermal Crystallization Behavior of PP/EVOH Blends

Polymer crystallization consists of nucleation and subsequent crystal growth. However, the nucleation of a crystallizable polymer may be caused by homogeneous or by heterogeneous particles (impurities, nucleating agent, fillers or others), which can control the microstructure and physical properties of the polymer. Therefore, the overall crystallization behavior of the polymer can be analyzed by observing the nucleation and growth of polymer crystals or the overall rate of crystallization.

Moreover, the overall crystallization behavior of the polymer can predict the relationship between the microstructures and the preparation conditions of the polymers. Non-isothermal crystallization exotherms of pure PP, PP-g-MAH, EVOH and PP/EVOH blends recorded at the cooling rate of 10 °C/min are shown in Fig. 3. The pure PP, PP-g-MAH, EVOH and EVOH-0 show a single exothermic peak and the crystallization temperature values of 110 °C, 103 °C and 160 °C, respectively. EVOH-5, EVOH-10 and EVOH-15 show two exothermic peaks. The crystallization peak of EVOH in blends changes from one peak to two peaks as the content of EVOH increases. Moreover, the crystallization temperature values of PP in PP/ EVOH blends shift to 119 °C. The time needed to reach the maximum of exothermic peak during non-isothermal crystallization decreases remarkably after the addition of EVOH. As we know, the exothermic peak corresponds to the rates of nucleation and growth of the polymer during non-isothermal crystallization. According to the above analysis, all PP/EVOH blends show a heterogeneous nucleation process implying that the EVOH essentially acts as an effective nucleating agent for PP matrix and promotes the crystallization rate of PP during non-isothermal crystallization. Thus, as EVOH content increases, the crystallization behavior of PP/EVOH blends change remarkably and an increase in crystallization temperature is observed.

3.3 Isothermal Crystallization Kinetics of PP/EVOH Blends

It has been reported that the existence of OH groups would seriously reduce the overall rate of crystallization (Gupta et al., 2013). However, based on the results of non-isothermal crystallization of PP/EVOH blends, the crystallization behavior of

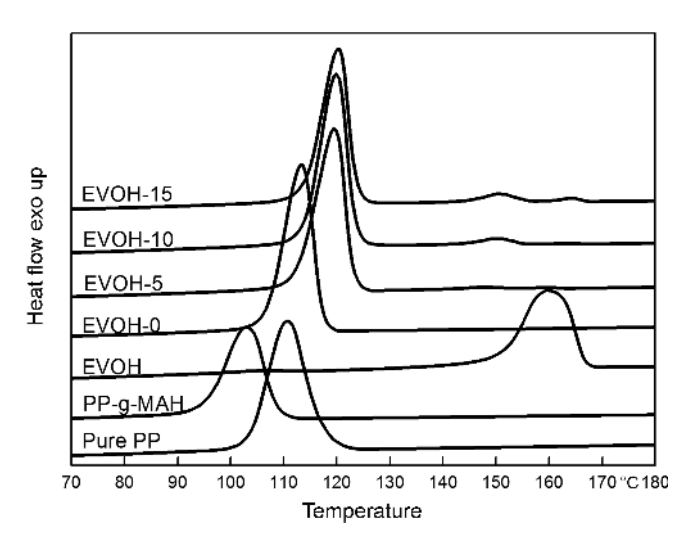


Fig. 3. Non-isothermal crystallization exotherms of PP/EVOH blends recorded at the heating/cooling rate of 10°C/min

PP/EVOH blends will be effected by EVOH. Thus, it is important to investigate the effect of EVOH content on the isothermal crystallization behavior of PP/EVOH blends in order to prepare hollow fiber membranes with three-dimensional circular structures.

Generally, the isothermal crystallization kinetics of polymers and polymer blends can be represented by the classical Avrami equation (Avrami, 1939; Avrami, 1940) as given in Eq. 1.

$$1 - X(t) = \exp(-Kt^n), \tag{1}$$

where n is the Avrami exponent that is associated with the mode of nucleation, crystal growth geometry and the type of growth process, K is the Avrami constant that provides the overall rate of crystallization. The fraction of X(t) is the relative crystallinity at time, t, defined as:

$$X(t) = \frac{X_c(t)}{X_c(t = \infty)} = \frac{\int_0^t (dH/dt)dt}{\int_0^\infty (dH/dt)dt} = 1 - exp(-Kt^n), \quad (2)$$

where (dH/dt) is the heat evolution rate during the crystallization process. Eq. 2 assumes that the heat released during crystallization is linearly proportional to the evolution of crystallinity. The K is governed by the mode of primary nucleation (heterogeneous or homogeneous) and the rate of radial growth (G) of the crystal. For m-dimensional crystal growth, K varies as follows:

$$K \propto NG^m$$
; Heterogeneous, (3)

$$K \propto IG^m$$
; Heterogeneous, (4)

where N is the number (or number density) of primary nuclei and I is the rate of primary nucleation. If the assumptions made by the Avrami formulation are valid, the form of Eq. 1 is invariant for all crystal geometries and growth kinetics. In order to deal conveniently with the operation, Eq. 1 can be rewritten as follows:

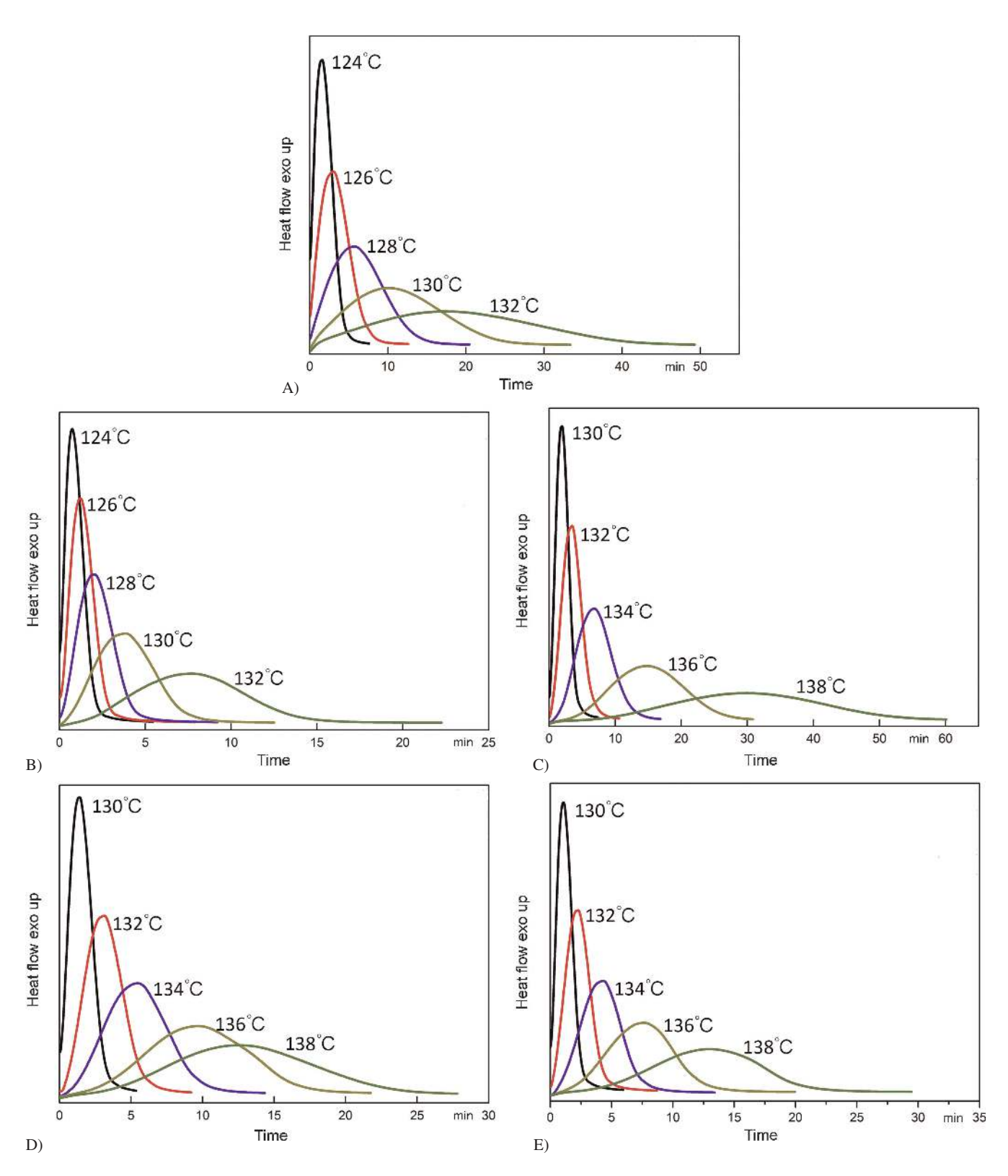
$$\log(-\ln(1 - X(t))) = \log K + n \log t. \tag{5}$$

According to Eq. 5, when plotting log(-ln(1-X(t))) against log t, the n and K values could be directly obtained as the slope and the antilogarithmic value of the y-intercept, respectively.

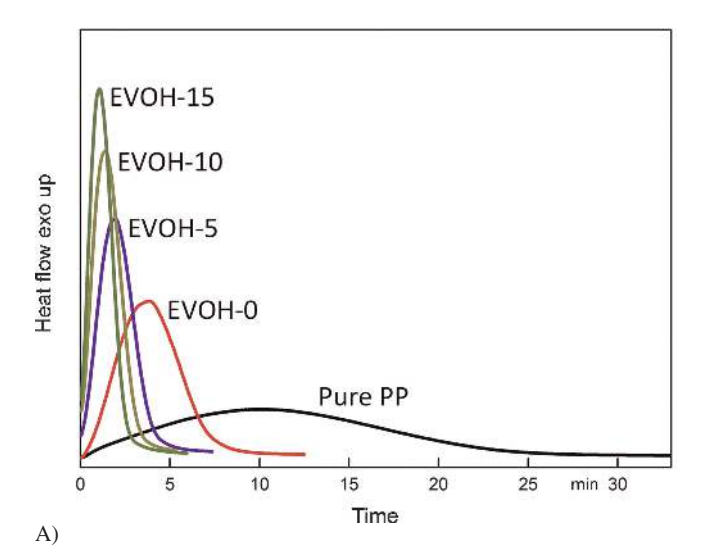
Based on the analysis of Fig. 1, the T_C of pure PP and EVOH-0 are set at 124, 126, 128, 130, and 132 °C. However, the T_C of EVOH-5, EVOH-10 and EVOH-15 are set at 130, 132, 134, 136, and 138 °C to more precisely study the effect of EVOH on the crystallization behavior of samples. The isothermal crystallization exotherms for all samples with different T_C are presented in Fig. 4. In general, the time required for the completion of crystallization decreases with decreasing T_C for all blends. Figure 4 indicates that the time to reach the maximum of the exothermic peak of isothermal crystallization, t_{max}, decreases as the EVOH content is increased. Meanwhile, crystallization exotherms of all samples at the crystallization temperature of 130 °C and 132 °C are given in Fig. 5 to more precisely compare the effect of EVOH on the crystallization behavior of blends. It can be seen from Fig. 5 that PP/EVOH blends have shorter time for finishing crystallization at the same T_C than pure PP, indicating that EVOH accelerates the crystallization of PP greatly. It is interesting to note that EVOH-0 also has shorter time for finishing crystallization than pure PP, indicating that PP-g-MAH may accelerate crystallization of PP. However, some scholars have reported that the nucleation of PP was not effected by the addition of PP-g-MAH (Xu et al., 2003; Wu et al., 2010; Wang et al., 2001; Wang et al., 2005). Therefore, the change of time might correspond to a heterogeneous nucleation due to the existence of impurities in the EVOH-0 blend.

Figure 6 shows the relative crystallinity versus crystallization time for pure PP and PP/EVOH blends. It is found that the relative crystallinity increases with increase of time. All the curves have similar sigmoidal shapes. The curvatures of the lower and upper parts of the curves are due to the formation of nuclei and the spherulitic crystal impingement in the later stages of crystallization, respectively (Ferreira et al., 2013).

The effect of EVOH content on the plot of log(-ln(1-X(t))) versus log t for PP/EVOH blends is shown in Fig. 7. The overall crystallization rate may be due to the change either in the crystal growth rate or in the nucleation rate. The kinetic parameters of the Avrami equation, such as n and K can be determined with the fit of the initial stage data (Wunderlich, 1976). The results of Fig. 7 and Table 2 show that the number of Avrami exponents, n, of isothermal crystallization of PP/ EVOH blends increase by addition of EVOH. For all samples, the slope of the plots remains unchanged until a higher degree of conversion is reached and show a single/major exponent, n. In this work, the Avrami exponents, of isothermal crystallization of pure PP and PP/EVOH blends are non-integer. The non-integer n value may be considered in the literature due to the crystal branching and/or two-stage crystal growth and/or mixed growth and nucleation mechanism (Wunderlich, 1976; Grenier et al., 1980; Mandelkern, 2004; Jonsson et al., 1990). The Avrami exponent of 2.21 \pm 0.04 for pure PP crystallized in all temperatures is consistent with a two-dimensional growth process (Gupta et al., 2014; Xu et al., 1998). Some scholars have reported n values in the range of 2 to 4 for PP blends (Wunderlich, 1976; Carfagna et al., 1984). The value of n for EVOH-0 is ca. 2.52 ± 0.17 . This might correspond to a hetero-



 $Fig.\ 4.\ Effect\ of\ EVOH\ content\ and\ crystallization\ temperature\ on\ the\ isothermal\ crystallization\ kinetics\ of\ pure\ PP\ and\ PP/EVOH\ blends:$ $A)\ pure\ PP,\ B)\ EVOH-0,\ C)\ EVOH-5,\ D)\ EVOH-1,\ E)\ EVOH-15$



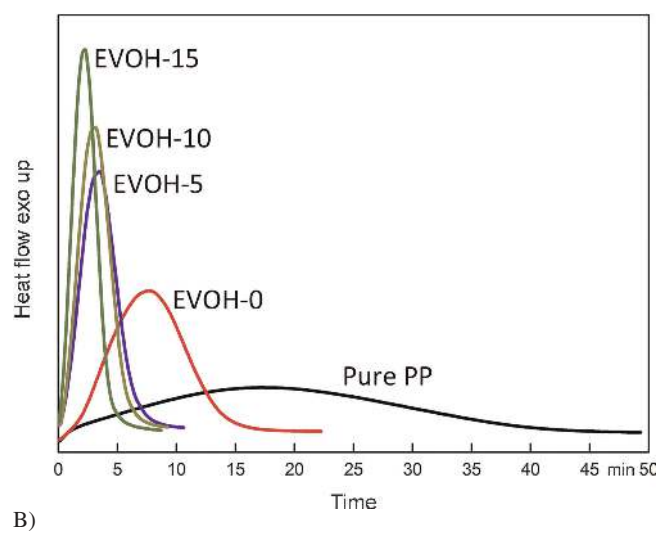


Fig. 5. Comparison of the crystallization exotherms of all samples at the same $T_C(A)$ 130°C and (B) 132°C

geneous nucleation due to the existence of impurities from the process of extrusion. n values close to 2.5 may hint a thermal nucleation process followed by mixing two-dimensional and three-dimensional crystal growth, respectively (Chen et al., 2007). In this work, the n values for EVOH-5, EVOH-10 and EVOH-15 are ca. 2.86 ± 0.22 , 2.80 ± 0.17 and 2.79 ± 0.25 respectively, indicating that the crystal growth pattern of PP changes to three-dimensional crystal growth after addition of EVOH. Because EVOH will crystallize first due to its higher crystallization temperature than that of PP, a two phase interface will be formed because the EVOH molecules in PP/EVOH blends aggregate to form the sea-island structure.

The Avrami constants, K, of all samples are listed in Table 2 and calculated from the Avrami plots in Fig. 7. For all samples, K decreases with the increase of $T_{\rm C}$, indicating that the nucleation and growth rate of the materials are falling with the increase of $T_{\rm C}$. In addition, K of PP/EVOH blends are higher than that of pure PP and increase with the increase of EVOH content at the same $T_{\rm C}$, indicating that the crystalliza-

tion rate is increased and the dependence of crystal growth on time is reduced by the addition of EVOH.

The time to reach 50% of relative crystallinity $(t_{1/2})$ is an indication of the crystallization rate of the polymer and it can be obtained from the curves in Fig. 4. $t_{1/2}$ represents the time to reach the maximum rate of heat flow and corresponds to the change over to a slower kinetic process due to impingement of adjacent spherulites (Bodor, 1991). Based on Eq. 1, $t_{1/2}$ can also be directly calculated as follows:

$$t_{1/2} = \left(\frac{\ln 2}{K}\right)^{1/n}. (6)$$

The time at maximum heat flow (t_{max}) can also be obtained directly from Fig. 4. Table 2 shows the value of $t_{1/2}$ and t_{max} of all samples. The result indicates that the $t_{1/2}$ and t_{max} of pure PP and PP/EVOH blends decrease with increase of EVOH content and decreasing of T_C . Addition of EVOH shortens $t_{1/2}$ and t_{max} of PP obviously, indicating that EVOH has high nucleation efficiency. Therefore, this fact clearly proves that the EVOH acts as an essential nucleating agent for PP and promotes nucleation rate of PP chains during isothermal crystallization.

If it is assumed that the crystallization process is thermally activated, the following Arrhenius equation can be used for calculating the crystallization activation energy (Cebe et al., 1986; Zhu et al., 2001).

$$K^{1/n} = K_0 \exp\left(-\frac{\Delta E}{RT_C}\right),\tag{7a}$$

or

$$\left(\frac{1}{n}\right) lnK = lnK_0 - \left(\frac{\Delta E}{RT_C}\right), \tag{7b}$$

where K₀ is a pre-exponential factor independent of temperature. R is the gas constant and the value is 8.32 J mol⁻¹ K⁻¹ (Naffakh et al., 2008). T_C is the isothermal crystallization temperature, and ΔE is the crystallization activation energy. Figure 8 shows the plots of (1/n)lnK versus 1/T_C for pure PP and PP/EVOH blends. A good linearity existing between (1/n)lnK versus 1/T_C can be seen in Fig. 8. The crystallization activation energy ΔE of pure PP and PP/EVOH blends can be calculated from the slope of the obtained straight lines, and the values are also represented in Table 2. It is known that the magnitude of the activation energy $|\Delta E|$ is related to the energy required for the movement of the polymer chains during the transition from the melt to the crystalline state. Higher $|\Delta E|$ means that this transition needs to release more energy suggesting a more difficult motion of polymer chains in the system (Li et al., 2007; Durmus et al., 2012). The $|\Delta E|$ s of PP/EVOH blends are lower than that of pure PP. The $|\Delta E|$ of EVOH-10 is minimum, and the $|\Delta E|$ of EVOH-15 is slightly increased. The main reason for this may be that the increase of two phase interface increases the number of nucleations. Meanwhile, the PP molecular chains will be hindered seriously if excessive amounts of EVOH are added. The obstruction leads to a decrease in the crystal growth rate despite an increase in the overall rate of crystallization.

Growth rate of spherulites, G, can be defined as $G = 1/t_{1/2}$, which is obtained from endotherm morphology of DSC analysis (Chen et al., 2007). The growth rate of crystallization can

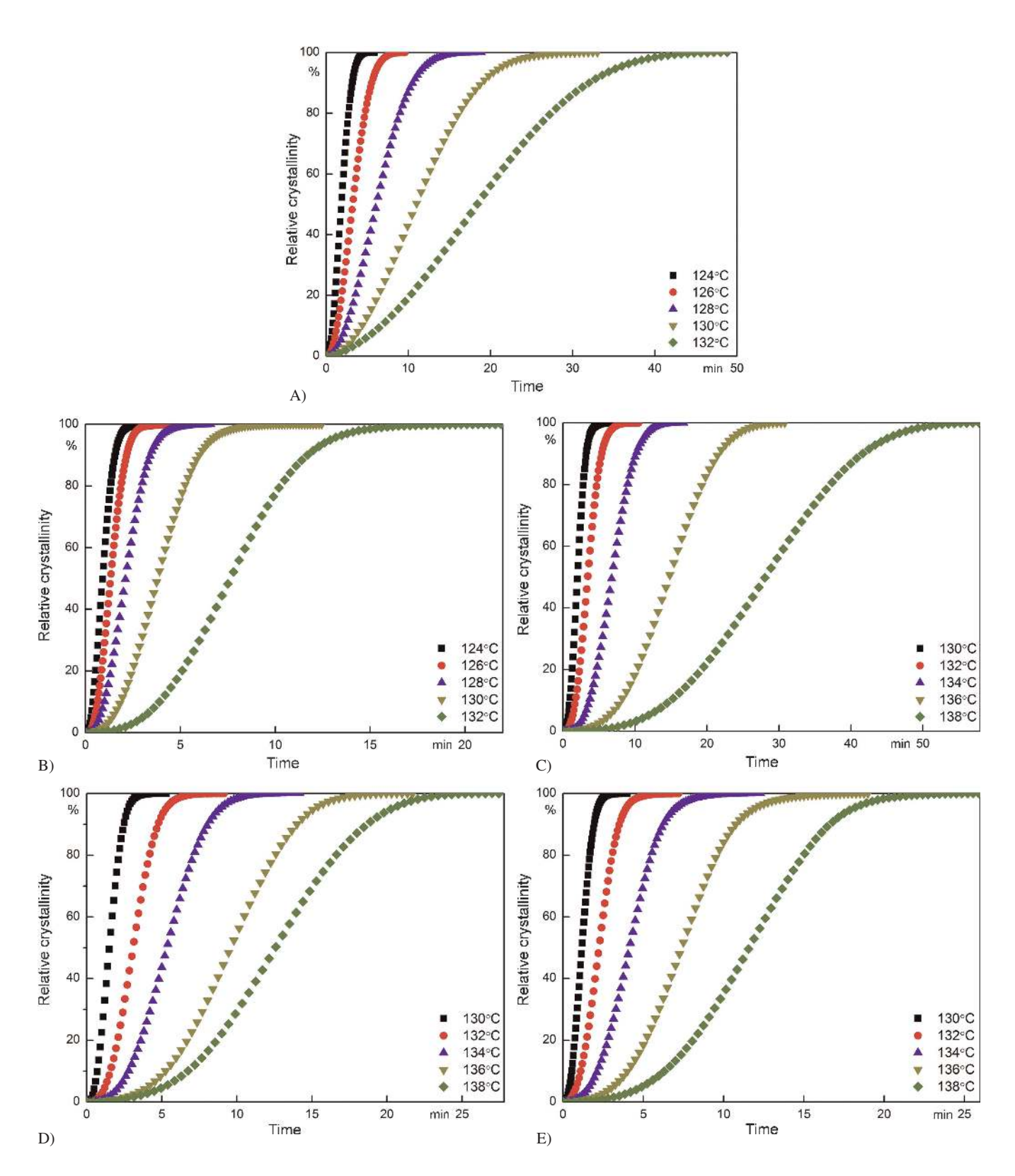


Fig. 6. Effect of EVOH content and crystallization temperature on the relative crystallinity of PP/EVOH blends: A) pure PP, B) EVOH-0, C) EVOH-10, E) EVOH-15

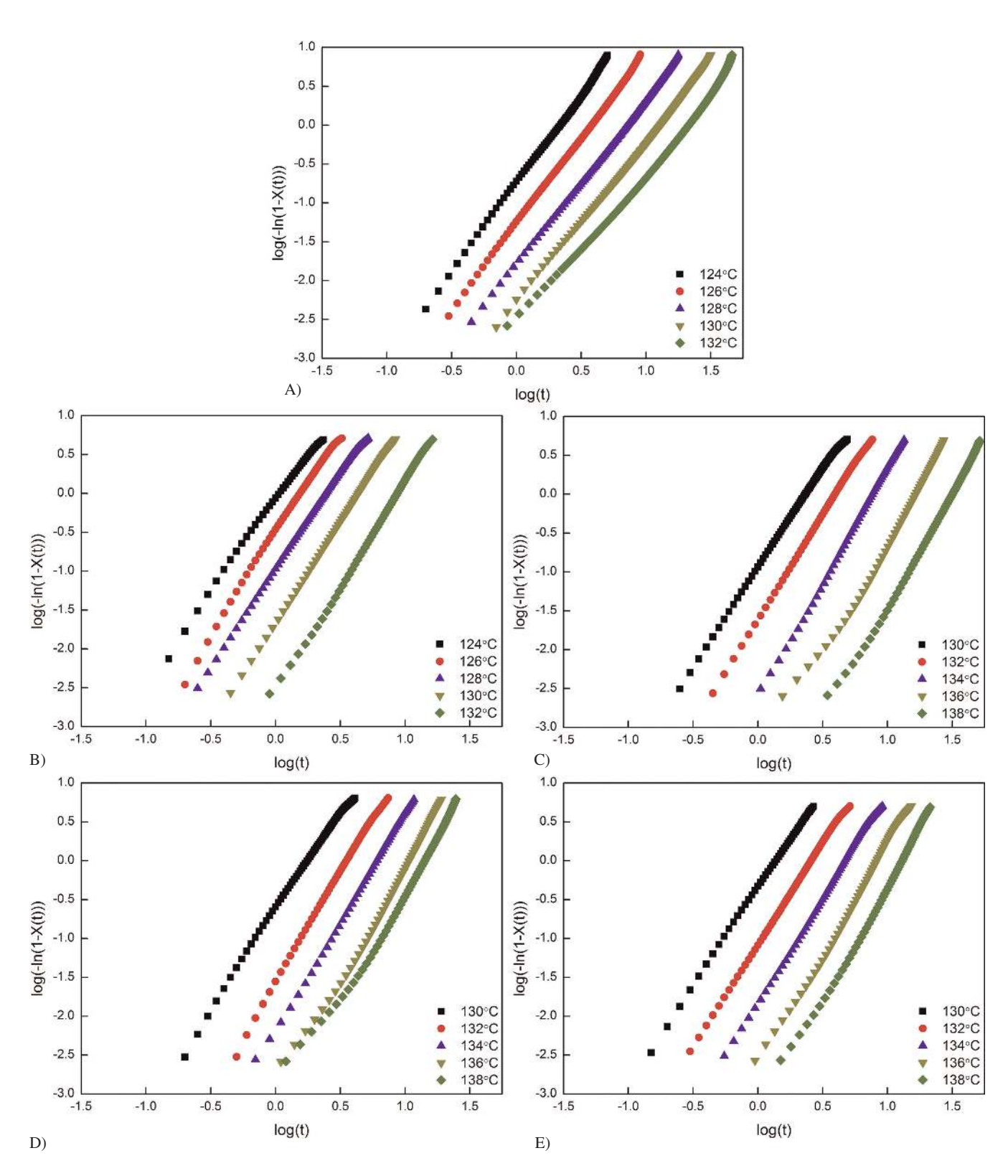


Fig. 7. Effect of EVOH content and crystallization temperature on the Avrami plots of pure PP and PP/EVOH blends: A) pure PP, B) EVOH-0, C) EVOH-10, E) EVOH-15

also be calculated with the isothermal crystallization data according to the Lauritzene-Hoffman secondary nucleation theory (Hoffman et al., 1976). Lauritzene-Hoffman theory consists of chain mobility and secondary nucleation terms. Crystal growth process is described as a combination of two processes; the deposition of the first stem on the growing crystal face (secondary nucleation) and the attachment of subsequent stems in the chain of the crystal surface (surface spreading process). There are three regimes as follows: In regime III, spherulite growth rate is governed by the rate of secondary nucleation. In regime II, spherulite growth rate is driven by both the rate of secondary nucleation and the rate of surface spreading. In regime I, the growth rate is the slowest since crystallization prevails at high temperatures (or under the condition of low undercooling) (Durmus et al., 2012). The n is equal to 4 for regime I (high temperatures) and III (low temperatures) and 2 in regime II (intermediate temperatures) (Hoffman, 1983). Lauritzene-Hoffman equation can be expressed as

$$G = G_0 exp \biggl[-\frac{U^*}{R(T_C - T_\infty)} \biggr] exp \biggl[-\frac{K_g}{T_C \Delta T f} \biggr], \eqno(8)$$

where G_0 is a pre-exponential factor; U^* is the energy required for the transport of macromolecules in the melt which is universally taken as 6.28 KJ/mol, T_C is the crystallization tem-

perature, T_{∞} is a hypothetical temperature where all the motions associated with the viscous flow stop which that is commonly defined as $T_g\text{--}30$ K, ΔT is the undercooling, defined as $\Delta T = T_m^0 - T_C$; f is a corrective factor for the decrease of

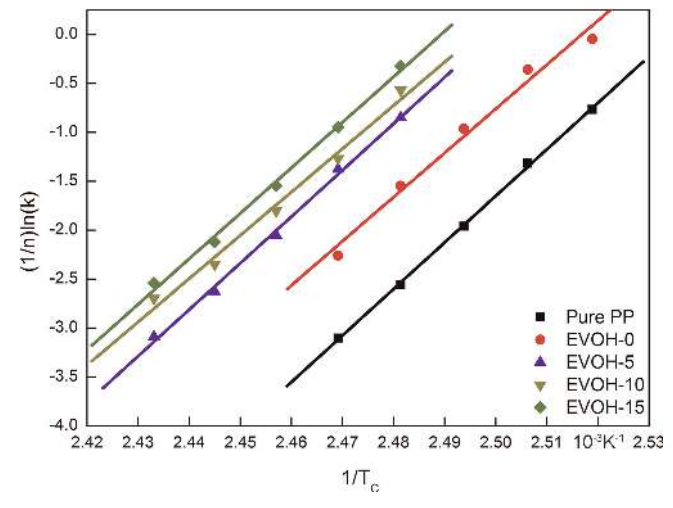


Fig. 8. Plots of (1/n)ln K versus $1/T_C$ for pure PP and PP/EVOH blends under isothermal crystallization

Sample	T _C °C	t _{1/2} min	t _{max} min	n	K °C/min	ΔE kJ/mol
PP	124	1.84	1.60	2.24	0.180	-396
	126	3.23	3.03	2.21	0.0546	
	128	6.11	5.70	2.15	0.0148	
	130	10.95	10.10	2.19	0.0037	
	132	18.38	17.20	2.26	0.0009	
EVOH-0	124	0.90	0.76	2.28	0.8279	-382
	126	1.33	1.22	2.56	0.3237	
	128	2.11	1.98	2.50	0.1060	
	130	3.80	3.84	2.53	0.0226	
	132	7.64	7.67	2.75	0.0018	
EVOH-5	130	2.01	1.87	2.55	0.1151	-395
	132	3.44	3.41	2.71	0.0241	
	134	6.78	6.81	2.96	0.0023	
	136	14.76	14.91	3.09	0.0002	
	138	30.31	29.84	2.98	0.0001	
EVOH-10	130	1.51	1.35	2.50	0.2416	-368
	132	3.09	3.08	2.81	0.0284	
	134	5.34	5.45	2.83	0.0061	
	136	9.60	9.65	2.94	0.0010	
	138	12.58	12.64	2.90	0.0005	
EVOH-15	130	1.18	1.08	2.47	0.4534	-386
	132	2.25	2.21	2.63	0.0827	
	134	4.14	4.30	2.78	0.0135	
	136	7.39	7.65	2.98	0.0018	
	138	11.60	12.96	3.08	0.0004	

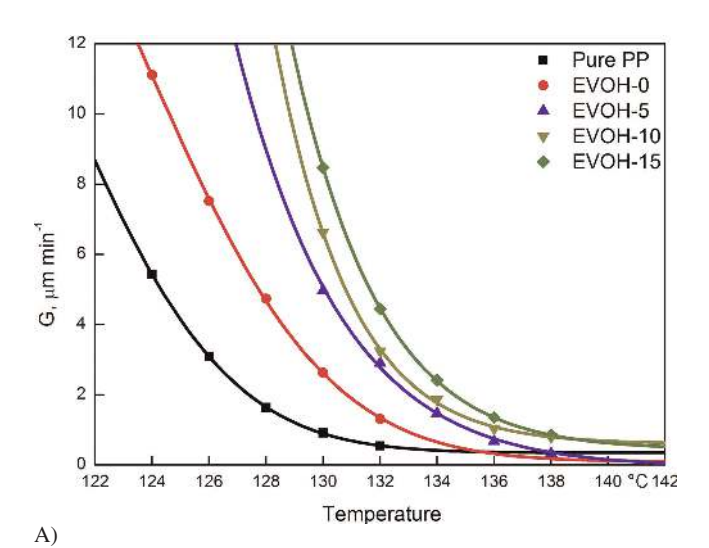
Table 2. The isothermal crystallization kinetics of PP/EVOH blends

the enthalpy of fusion with the crystallization temperature, $f=2T_C/\big(T_C+T_m^0\big).$ K_g is the nucleation parameter related to the fold and lateral surface energies, defined as $nb\sigma b_eT_m^0\big/\Delta H_m^0K.$ Lauritzene-Hoffman equation can be linearized as the following form by performing the logarithmic transformation;

$$lnG + \frac{U^*}{R(T_C - T_\infty)} = lnG_0 - \frac{K_g}{T_C \Delta T f}.$$
 (9)

Plots of $\ln G+U^*/R(T_C-T_\infty)$ against the term $1/T_C\Delta Tf$ of pure PP and PP/EVOH blends are shown in Fig. 9B. All the samples yielded no change in slope. This linearity indicates that no regime transition occurs in the crystallization for the temperature range employed.

The effect of EVOH content and crystallization temperature on the spherulite radial growth rate, G, during isothermal crystallization is given in Fig. 9A. The radial growth rate decreases with the increase of T_C for all the samples. The radial growth



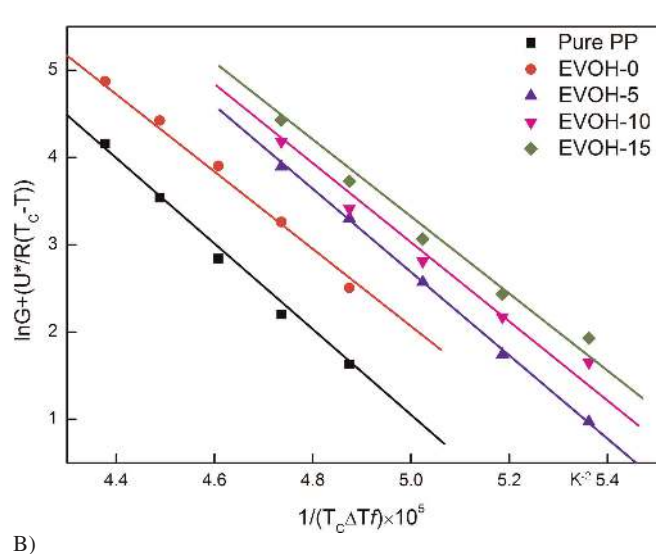


Fig. 9. Effect of EVOH contents and crystallization temperature on the spherulite radial growth rate, G, during isothermal crystallization

rate of PP matrix increases with the increase of the EVOH contents for all the samples at temperature below 138 °C. However, the G of EVOH-5 is gradually below than that of pure PP at more than 138 °C. The EVOH-15 also shows lower G value than EVOH-10 at more than 138 °C. It indicates that the addition of EVOH molecules can both influence the terms of formation of the critical nuclei and transportability of the PP chain in melt region during crystallization. The prosperity of G at lower crystallization temperature confirms that the accelerated formation of the critical nuclei in the melt is the factor that dominates the crystallization process of the PP/EVOH blends. The transportability of the PP chain is hindered by EVOH in melt region at higher crystallization temperature which is the factor that dominates the crystallization process. All the results indicate the addition of EVOH hinders the mobility of PP chain. However, the addition of EVOH changes the nucleation mechanism of PP and also significantly improves the nucleation rate of PP. Therefore, the overall rate of crystallization is still increasing.

3.4 Melting Behavior of Isothermally Crystallized PP/EVOH Blends

The melting behavior of isothermally crystallized PP/EVOH blends at different EVOH contents and $T_{\rm C}$ are given in Fig. 10. As can be seen from the Fig. 10A and B, the melting curves of pure PP and EVOH-0 show a single melting endotherm at 167 °C. The melting profiles of PP/EVOH blends show two melting endotherms at 168 °C and 188 °C, respectively. However, for all the samples, PP component exhibits a single melting endotherm indicating that the crystal forms of PP are not affected by EVOH. Figure 10 also shows that the peak temperature, $T_{\rm pm}$, linearly increases with the isothermal crystallization temperature for all samples. Thus, the Hoffmann-Weeks equation is used to determine the equilibrium melting temperature, $T_{\rm m}^{\rm m}$ (Hoffman et al., 1965); a plot of $T_{\rm C}$ versus $T_{\rm m}$ with a line is drawn where $T_{\rm C}=T_{\rm m}$. The experimental data can be extrapolated to the intersection with the line, which is the equilibrium melting temperature, $T_{\rm 0}$:

$$T_{m}^{0} - T_{m} = \phi' (T_{m}^{0} - T_{C}), \tag{10}$$

where ϕ^\prime represents a stability parameter that depends on crystal size and perfection. Figure 11 indicates the melting temperatures registered at the T_{pm} versus different T_C for the isothermally crystallized PP/EVOH blends. A straight line is extrapolated from the experimental T_{pm} values of PP/EVOH blends with different T_C , and the calculated T_m^0 for all PP/ EVOH blends is observed. Figure 11 shows the effect of EVOH content on the T_m^0 of PP/EVOH blends. The results show that the T_m^0 values are dramatically higher than that of pure PP. Generally, the perfection of the crystalline, or hightemperature melting peaks increases with crystallization temperature. Therefore, the increase of T_m⁰ values of PP/EVOH blends can be explained from the following two aspects. First, the EVOH acts as an essential nucleating agent for PP and promotes nucleation of PP chains during isothermal crystallization. The more perfect crystals may be formed. Also, the test temperature of PP/EVOH blends is higher than that of

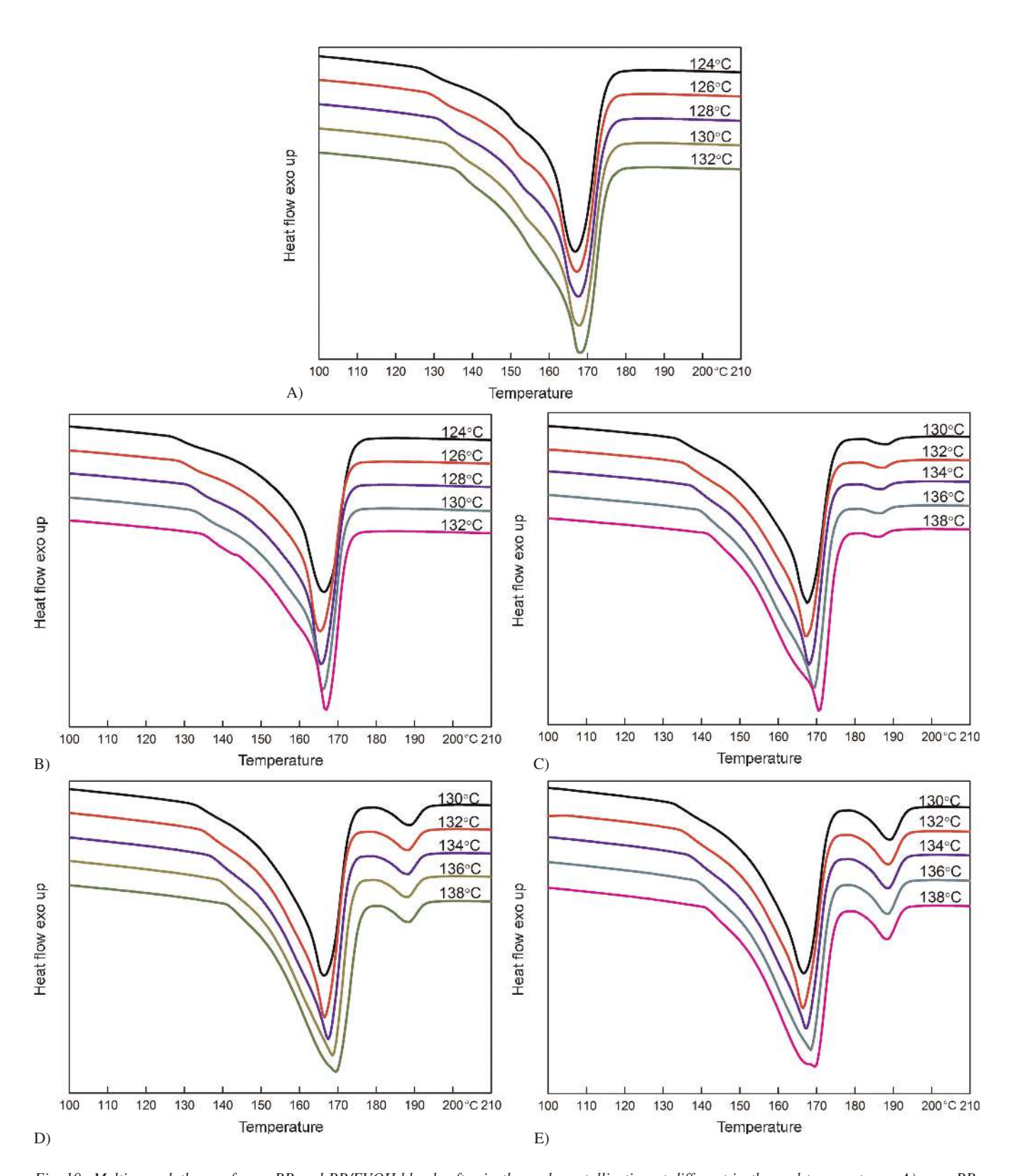


Fig. 10. Melting endotherm of pure PP and PP/EVOH blends after isothermal crystallization at different isothermal temperatures: A) pure PP, B) EVOH-0, C) EVOH-5, D) EVOH-1, E) EVOH-15

pure PP. It is also easier to form more perfect crystals at high temperature. In addition, the T_m^0 values of PP/EVOH blends decrease slightly with the increase of EVOH content, because the excessive amounts of EVOH led to a serious retardation of the mobility of PP chains in the melted state, and so a imperfect crystal is formed at higher EVOH content. These values

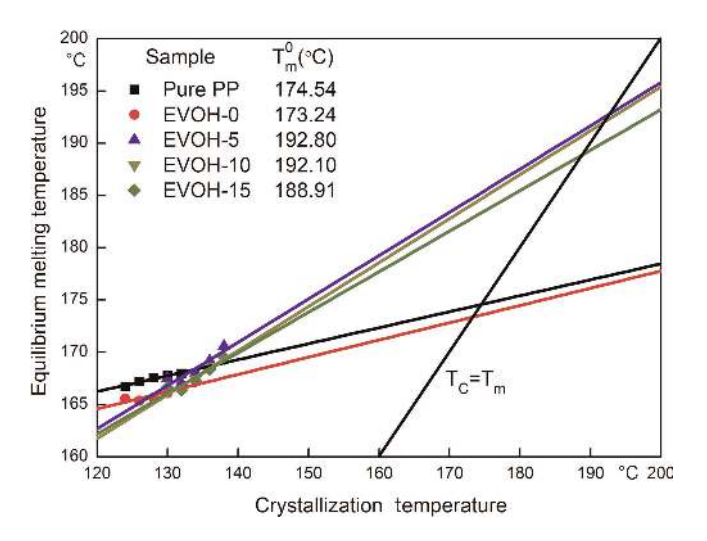


Fig. 11. Plot of the observed equilibrium melting temperature, T_m^0 , by linearly increasing the melting temperature of the peak temperature, T_{pm} , for pure PP and PP/EVOH blends with the crystallization temperature, $1/T_C$ recorded using the linear Hoffman-Weeks extrapolation

confirm the previous conclusion that the EVOH content has a significant effect on the crystallization behavior of PP.

3.5 Morphology and Microstructure of PP/EVOH Blends

The crystal size markedly affects the performance of hollow fiber membranes by MSCS. To investigate the influence of EVOH on the size of spherulites of PP, we performed polarized light microscopy (PLM) experiments on both pure PP and EVOH-10 blend as shown in Fig. 12. For pure PP, the crystal aggregates are three-dimensional spherulites comprising crystals growing in two dimensions (n = 2), which is consistent with the DSC results. In addition, the common spherulitic superstructures are observed in pure PP. All the spherulites show similar sizes with approximately 100 µm in diameter after complete crystallization. Comparably, the morphology development of spherulites for EVOH-10 shows the instantaneous nucleation process followed by a three- and two-dimensional crystal growth as shown in Fig. 12B during crystallization. In addition, no defined superstructures of crystallites are discerned in EVOH-10 after complete crystallization. The crystallization time of PP matrix is shortened by addition of EVOH, which is consistent with the isothermal crystallization kinetics results. In addition, the introduction of EVOH leads to a substantial decrease in the spherulite size of PP and the nucleation density of EVOH-10 is higher than that of PP. This is because the presence of heterogeneities reduces the barrier to nucleation caused by the surface interfacial free energy (Mandelkern, 2004). It leads to an increased number of nucleation sites which, ultimately, reduces the size of the spherulites due

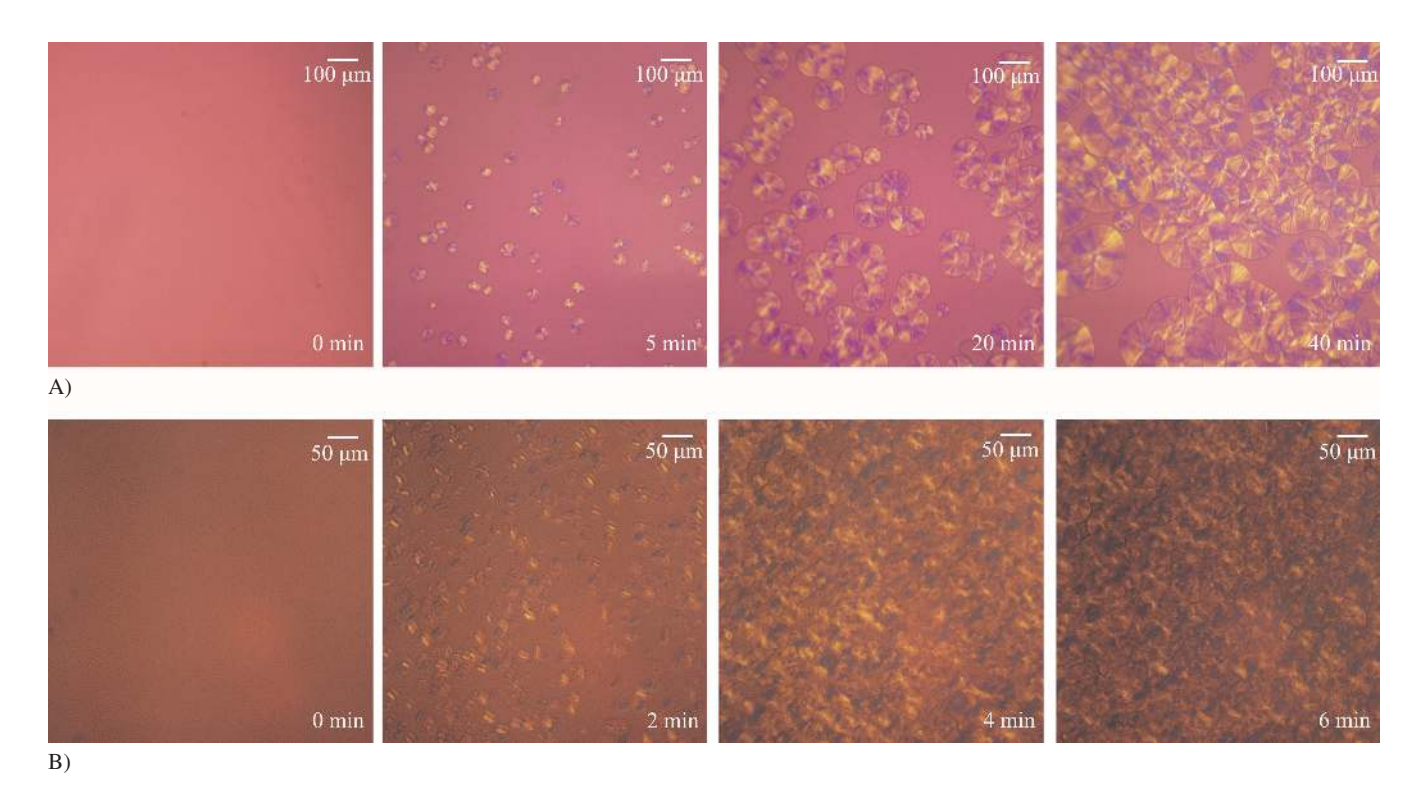


Fig. 12. Development of crystal morphology with time for the isothermal crystallization of pure PP (A) and EVOH-10 (B) at 155 °C

to impingement of the spherulites with one another and with the EVOH crystals. The spherulites superstructures cannot be observed when the density of heterogeneities is very high.

The crystal form also markedly affects the performance of hollow fiber membranes by MSCS. In order to study the crystal form of PP in blends in detail, XRD analysis was used to investigate the crystal form change of PP/EVOH blends. Figure 13 shows the XRD intensity profiles of PP/EVOH blends after isothermal crystallization at 155 °C. The reflection for all samples appears at $2\theta = 14.0^{\circ}$, 16.8° , 18.5° , 21.7° , 25.4° , and 16.0° corresponding to the planes (110), (040), (130), (131), and (060) of α -crystal and the plane (300) of β -crystal, respectively. In general, no β -crystal exists in pure PP but is observed here. Eventually, during injection molding, the oriented β -crystals with their c-axis perpendicular to the injection molding direction were formed (Chen et al., 2016; Jiang et al., 2015). These X-ray diffractograms of PP/EVOH blends confirm that the ad-

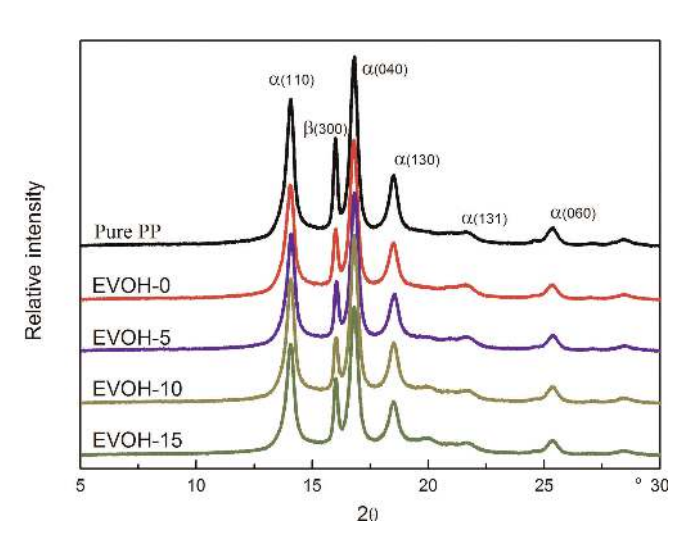


Fig. 13. XRD intensity patterns of PP/EVOH blends

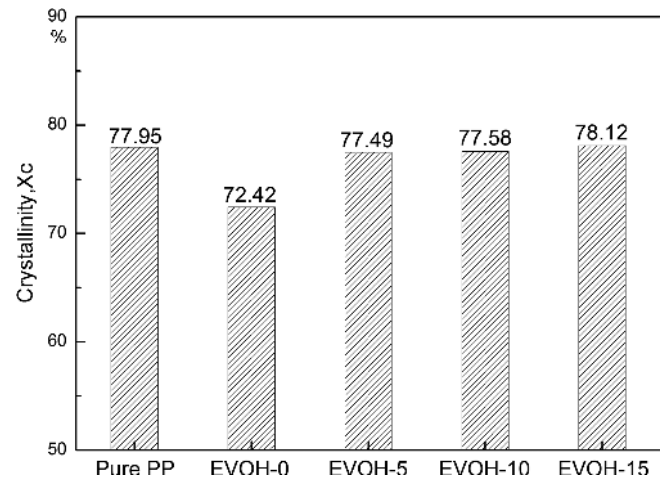


Fig. 14. Effect of EVOH content on the crystallinity of PP/EVOH blends

dition of EVOH does not affect the crystalline polymorphy of PP matrix.

In general, high-performance hollow fiber membrane can be obtained by increasing crystallinity. Figure 14 represents the crystallinity of PP phase in PP/EVOH blends. The crystallinity of EVOH-0 is slightly lower than that of pure PP. The addition of PP-g-MAH did not affect the nucleation of PP, but PP-g-MAH would hinder the PP molecular chain into the lattice (Wang et al., 2001; Wang et al., 2005). Therefore, the crystallinity will be reduced. However, the crystallinity of PP phase in EVOH-5, EVOH-10, and EVOH-15 are not significantly different from that of pure PP. The main reason is that the EVOH essentially acts as an effective nucleating agent for PP matrix and promotes the crystallization of PP, but the increase of EVOH content will hinder the mobility of PP chains in the melted state and reduce the PP chain to allow the recrystallization to takes place. Therefore, as the EVOH content increases, the crystallinity of PP in blends does not increase further.

4 Conclusions

In this work, PP/EVOH blends were prepared by melt blending using PP-g-MAH as a compatibilizer. The effect of EVOH on microstructure, rheological behavior and isothermal crystallization behavior of PP phase in PP/EVOH blends were investigated. The EVOH particles were uniformly dispersed in the PP matrix and inhibited the mobility of PP chains. The values of Avrami exponent n were increased from 2.21 for PP to 2.86, suggesting a three-dimensional crystal growth mechanism with heterogeneous nucleation. The overall rate of crystallization of PP/EVOH blends was higher than that of pure PP and increased with the increase of EVOH content at the same T_C . However, the $|\Delta E|$ of EVOH-10 was minimum and the $|\Delta E|$ of EVOH-15 was slightly higher, indicating that the PP molecular chains would be hindered seriously if excessive amounts of EVOH were added. The PLM observations revealed the decreased size and increased nucleation density of PP spherulites due to nucleating effect of EVOH. In addition, X-ray diffraction results indicated that the addition of EVOH did not change the overall crystalline structure or decrease the crystallinity of PP. Therefore, we could conclude that EVOH essentially acted as an effective nucleating agent for PP. The introduction of EVOH increased the overall rate of isothermal crystallization compared with pure PP, although the crystal growth rate would decrease if excessive amounts of EVOH were added. The EVOH-10 appeared to be promising to reduce the impact on the crystallization of PP in order to generate the desired structure. Future publications on these blends will address hollow fiber membranes preparation and the three-dimensional circular structure form of these PP/EVOH blends.

References

Avrami, M., "Kinetics of Phase Change. I General Theory", J. Chem. Phys., 7, 1103–1112 (1939), DOI:10.1063/1.1750380

Avrami, M., "Kinetics of Phase Change. II Transformation-Time Relations for Random Distribution of Nuclei", J. Chem. Phys., **8**, 212–224 (1940), DOI:10.1063/1.1750631

- Baker, R. W.: Membrane Technology and Applications, 2nd Edition, John Wiley & Sons Manhattan (2004), DOI:10.1002/0470020393
- Bodor, G.: Structural Investigation of Polymers, Ellis Horwood, Chichester, England (1991)
- Carfagna, C., Derosa, C., Guerra, G. and Petraccone, V., "Brushless Planetary Gearmotors (Motion Products Positioning Devices)", Polymer, 25, 1462–1464 (1984), DOI:10.1016/0032-3861(84)90110-1
- Cebe, P., Hong, S. D., "Crystallization Behavior of Poly(ether ether ketone)", Polymer, 27, 1183–1192 (1986), DOI:10.1016/0032-3861(86)90006-6
- Chen, J. H., Yao, B. X., Su, W. B. and Yang, Y. B., "Isothermal Crystallization Behavior of Isotactic Polypropylene Blended with Small Loading of Polyhedral Oligomeric Silsesquioxane", Polymer, 48, 1756–1769 (2007), DOI:10.1016/j.polymer.2007.01.010
- Chen, Y. H., Yang, S., Yang, H. Q., Zhong, G. J., Fang, D. F., Hsiao, B. S. and Li, Z. M., "Deformation Behavior of Oriented β-Crystals in Injection-Molded Isotactic Polypropylene by in situ X-Ray Scattering", Polymer, 84, 254–266 (2016), DOI:10.1016/j.polymer.2016.01.004
- Durmus, A., Kasgoz, A., Ercan, N., Akın, D., Şanlı, S., "Effect of Polyhedral Oligomeric Silsesquioxane (POSS) Reinforced Polypropylene (PP) Nanocomposite on the Microstructure and Isothermal Crystallization Kinetics of Polyoxymethylene (POM)", Polymer, 53, 5347–5357 (2012), DOI:10.1016/j.polymer.2012.09.026
- Fan, Q. C., Duan, F. H., Guo, H. B. and Wu, T., "Non-isothermal Crystallization Kinetics of Polypropylene and Hyperbranched Polyester Blends", Chinese J. Chem. Eng., 23, 441–445 (2015), DOI:10.1016/j.cjche.2014.11.016
- Ferreira, C. I., Castel, C. D., Oviedo, M. A. S. and Mauler, R. S., "Isothermal and Non-Isothermal Crystallization Kinetics of Polypropylene/Exfoliated Graphite Nanocomposites", Thermochim. Acta, 553, 40–48 (2013), DOI:10.1016/j.tca.2012.11.025
- Grenier, D., Homme, R. E. P., "Avrami Analysis: Three Experimental Limiting Factors", J. Polym. Sci., Part B: Polym. Phys, 181, 655– 1657 (1980), DOI:10.1002/pol.1980.180180715
- Gupta, S., Yuan, X. P., Chung, T. C. M., Cakmak, M. and Weiss, R. A., "Isothermal and Non-Isothermal Crystallization Kinetics of Hydroxyl-Functionalized Polypropylene", Polymer, **55**, 924–935 (2014), DOI:10.1016/j.polymer.2013.12.063
- Gupta, S., Yuan, X., Chung, T. C. M., Kumar, S., Cakmak, M. and Weiss, R. A., "Effect of Hydroxyl-Functionalization on the Structure and Properties of Polypropylene", Macromolecules, 46, 5455–5463 (2013), DOI:10.1021/ma4008658
- Hoffman, D. J., "Regime III Crystallization in Melt-Crystallized Polymers: The Variable Cluster Model of Chain Folding", Polymer, 24, 3–26 (1983), DOI:10.1016/0032–3861(83)90074-5
- Hoffman, D. J., Davis, G. T. and Lauritzen, J. L.: Treatise on Solid State Chemistry, Volume 3, Crystalline and Non-Crystalline Solids, Plenum Press, New York (1976)
- Hoffman, D. J., Weeks, J. J., "X-Ray Study of Isothermal Thickening of Lamellae in Bulk Polyethylene at the Crystallization Temperature", J. Chem. Phys., **42**, 4301–4302 (1965), DOI:10.1063/1.1695935
- Jiang, J., Wang, S. W., Sun, B., Ma, S. J., Zhang, J. M., Li, Q. and Hu, G. H., "Effect of Mold Temperature on the Structures and Mechanical Properties of Micro-Injection Molded Polypropylene", Mater. Des., 88, 245–251 (2015), DOI:10.1016/j.matdes.2015.09.003
- Jonsson, H., Wallgren, E., Hult, A. and Gedde, U. W., "Kinetics of Isotropic-Smectic Phase Transition in Liquid-Crystalline Polyethers", Macromolecules, 23, 1041–1047 (1990), DOI:10.1021/ma00206a022
- Li, J., Fang, Z., Zhu, Y., Tong, L., Gu, A. and Liu, F. M., "Isothermal Crystallization Kinetics and Melting Behavior of Multiwalled Carbon Nanotubes/Polyamide-6 Compsites", J. Appl. Polym. Sci., 105, 3531–3542 (2007), DOI:10.1002/app.24606
- Li, N. N., Xiao, C. F., Mei, S. and Zhang, S. J., "The Multi-Pore-Structure of Polymer-Silicon Hollow Fiber Membranes Fabricated via Thermally Induced Phase Separation Combining with Stretching", Desalination, 274, 284–291 (2011), DOI:10.1016/j.desal.2011.03.020
- Mandelkern, L.: Crystallization of Polymers Kinetics and Mechanisms, 2, Cambridge University Press, Cambridge (2004), DOI:10.1017/CBO9780511535413

- Mei, L., Zhang, D. S. and Wang, Q. R., "Morphology Structure Study of Polypropylene Hollow Fiber Membrane Made by the Blend-Spinning and Cold-Stretching Method". J. Appl. Polym. Sci., 84, 1390–1394 (2002), DOI:10.1002/app.10280
- Naffakh, M., Martín, Z., Marco, C., Gómez, M. A. and Jiménez, I., "Isothermal Crystallization Kinetics of Isotactic Polypropylene with Inorganic Fullerene-like WS₂ Nanoparticles", Thermochim. Acta, **472**, 11–16 (2008), DOI:10.1016/j.tca.2008.03.003
- Saffar, A., Carreau, P. J., Ajji, A. and Kamal, M. R., "Development of Polypropylene Microporous Hydrophilic Membranes by Blending with PP-g-MA and PP-g-AA", J. Membr. Sci., 46, 250–261 (2014), DOI:10.1016/j.memsci.2014.03.024
- Wang, D. Q., Ma, J. H. and Liang, B. R., "Crystallization Kinetics and Morphology of PP/PP-g-MAH/Org-MMT Nanocomposite", Polym. Mater. Sci. Eng., 21, 125–128 (2005)
- Wang, K., Wu, J. S. and Zeng, H. M., "Effect of Interfacial Interaction on Rheological and Crystalline Behavior of Polypropylene/BaSO₄ Composites", Acta Polym. Sin., 6, 697–701 (2001)
- Wu, N. J., Yang, P., "Crystallization and Phase Morphology of PP/ PMMA/PP-g-MAH Blends", Acta Polym. Sin., 3, 316–323 (2010), DOI:10.3724/SP.J.1105.2010.00316
- Wunderlich, B.: Macromolecular Physics, Volume 1, Academic Press, New York (1976)
- Wunderlich, B.: Macromolecular Physics, Volume 2, Academic Press, New York (1976)
- Xu, J., Srinivas, S., Marand, H. and Agarwal, P., "Equilibrium Melting Temperature and Undercooling Dependence of the Spherulitic Growth Rate of Isotactic Polypropylene", Macromolecules, 31, 8230–8242 (1998), DOI:10.1021/ma980748q
- Xu, W. B., Liang, G. D., Zhai, H. B., Tang S. P., Hang, G. P. and Pan, W. P., "Preparation and Crystallization Behavior of PP/PP-g-MAH/Org-MMT Nanocomposite", Eur. Polym. J., 39, 1467–1474 (2003), DOI:10.1016/S0014-3057(03)00015-6
- Zhang, Y. F., Chen, H., Liu, B. B., Gu, Y. H. and Li X. X., "Isothermal and Non-isothermal Crystallization of Isotactic Polypropylene Nucleated with 1,3,5-Benzenetricarboxylic Acid Tris(cyclohexylamide)", Thermochim. Acta, 590, 226–231 (2014), DOI:10.1016/j.tca.2014.07.007
- Zhou, H. M., Ying, J. R., Liu, F., Xie, X. L. and Li, D. Q., "Non-Isothermal Crystallization Behavior and Kinetics of Isotactic Polypropylene/Ethylene-octene Blends. Part I: Crystallization Behavior", Polym. Test., 29, 640–647 (2010), DOI:10.1016/j.polymertesting.2010.05.002
- Zhu, X. Y., Yan, D. Y., "Influence of the Order of Polymer Melt on the Crystallization Behavior: II. Crystallization Kinetics of Isotactic Polypropylene", Colloid. Polym. Sci., 279, 546–553 (2001), DOI:10.1007/s003960000449

Acknowledgements

This work was supported by the Guizhou science and technology plan project [Grant number [2017]2808]; and the Guizhou science and technology plan project [Grant number [2017] 2015].

Date received: September 21, 2017 Date accepted: June 20, 2018

Bibliography DOI 10.3139/217.3589 Intern. Polymer Processing XXXIV (2019) 2; page 195–208 © Carl Hanser Verlag GmbH & Co. KG ISSN 0930-777X